Effect of the degree of porosity on the performance of poly(vinylidene fluoride-trifluoroethylene)/poly(ethylene oxide) blend membranes for lithium-ion battery separators

A. Gören[1,2], C. M. Costa[1,*], M.N. Tamaño Machiavello[3], D. Cíntora-Juárez[4], J. Nunes-Pereira[1], J. L. Tirado[4], M. M. Silva[2], J. L. Gomez Ribelles[3,5] and S. Lanceros-Méndez[1*]

1- Centro/Departamento de Física, Universidade do Minho, 4710-057 Braga, Portugal.
2 - Centro/Departamento de Química, Universidade do Minho, 4710-057 Braga, Portugal.
3 - Center for Biomaterials and Tissue Engineering, CBIT, Universitat Politècnica de València, 46022 Valencia, Spain.
4 - Laboratorio de Química Inorgánica, Universidad de Córdoba, Edificio Marie Curie, Campus de Rabanales, 14071 Córdoba, Spain
5 - Networking Research Center on Bioengineering, Biomaterials and Nanomedicine (CIBER-BBN), Valencia, Spain

Corresponding author: cmscosta@fisica.uminho.pt; lanceros@fisica.uminho.pt

Abstract:

Porous polymer membranes based on poly(vinylidene fluoride-trifluoroethylene)/poly(ethylene oxide) copolymers, P(VDF-TrFE)/PEO, are prepared through the, from partial to total, elimination of PEO, leading to interconnected micropores in the polymer blends.

The electrolyte uptake, thermal and mechanical properties depends on the amount of PEO present in the polymer blend. Also the degree of crystallinity of PEO polymer and elastic modulus (E´) of the polymer blend decreases with increasing of PEO removal.

Electrical properties of the polymer blend membranes are influenced by the porosity and are dominated by diffusion. The temperature dependence of ionic conductivity follows the Arrhenius behavior. It is the highest for the membranes with a volume fraction of pores of 44% (i.e, 90% PEO removal), reaching a value of 0.54 $mS.cm^{-1}$ at room temperature.

Battery performance was determined by assembling Li/C-$LiFePO_4$ swagelok cells. The polymer blend with 90% PEO removal exhibit rate (124 $mAhg^{-1}$ at C5 and 47 $mAhg^{-1}$ at 2C) and cycling capabilities suitable for lithium ion battery applications.

1. Introduction:

Rechargeable Li-ion batteries, the ones most intensively studied for applications such as computers, mobile phones and electric vehicles, among others, due their outstanding properties: they are lighter and cheaper than other battery types, show high specific energy (100-265 Wh/Kg) and suitable power/weight relation (1800 W/Kg) [1, 2].

The main goal of the different investigations is to obtain the maximum energy density per unit of weight or volume taking into account its safety [3-5].

One essential component in Li-ion batteries is the polymer electrolyte (PE) consisting of a macromolecular system (polymer with salts in its constitution [6]) with high ionic conductivity ($>10^{-7}$ at 10^{-1} S/cm) [7, 8]. Further, polymer electrolytes can be used in multiple applications, including electrochromic devices [9-11], fuel cells [12, 13] and sensors/actuators [14], supercapacitors/ultracapacitors [15], together with Li-ion batteries [4, 16].

Solid polymer electrolytes (SPE) [8], gel polymer electrolytes (GPE) [17] and composite polymer electrolytes (CPE) [18] are different types of polymer electrolytes (PEs).

The SPE are the ones with the simplest fabrication, and, for Li-ion battery applications, consist in different lithium salts dissolved in a polymeric matrix. CPE are very similar to SPE but differs in the inclusion of different nanofillers (inert oxide ceramic, molecular sieves, metallic, carbonaceous fillers, ferroelectric materials) dispersed in the polymer matrix to improve the mechanical, thermal and electrochemical properties. The GPE are obtained in two steps, first the salts are dissolved in a polar or ionic liquid and then added to a host polymer to provide an adequate mechanical stability [19, 20].

In the area of battery applications, the separator/electrolyte are extremely important as they separate both electrodes (anode and cathode), control the number of ions and allow the movement of the ions between the electrodes during the charge and discharge process of the battery [21].

The main parameters of a separator/electrolyte are permeability, porosity/pore size, electrolyte absorption and retention, low ionic strength, mechanical and thermal stability, resistance to chemical degradation by electrolyte impurities and uniform thickness [16, 21].

Different polymers such as poly(ethylene oxide) (PEO) [22] and poly(acrylonitrile (PAN) [23] can be used as battery separators. Among the most interesting polymers for

this application are the highly polar and piezoelectric fluorinated polymers: poly(vinylidene fluoride) (PVDF) and their copolymers poly(vinylidene fluoride-*co*-trifluoroethylene), P(VDF-TrFE); poly(vinylidene fluoride-*co*-hexafluoropropene), P(VDF-HFP) and poly(vinylidene fluoride-*co*-chlorotrifluoroethylene), P(VDF-CTFE) [16].

For battery separator, these fluorinated polymers show strong advantages in comparison to other polymers (such as polyolefins) as they show high dipolar moment and dielectric constant which are important to increase lithium salts ionization, semi-crystallinity, chemical resistance, suitable mechanical strength, possibility of porosity control through binary and ternary polymer/solvent systems and high anodic stability due to the presence of strong electron-withdrawing function groups (-C-F-) [16, 24, 25].

In particular, P(VDF-TrFE) has excellent properties to be used as battery separator in lithium ion battery applications, as sample preparation varying polymer/solvent ratio allows to vary the degree of porosity, which is correlated to electrolyte uptake and ionic conductivity [25].

Polymer blends are often used as battery separator in lithium ion battery applications when the polymers that compose the blend show complementary properties that allow improving separator performance. For example, it is typical the use of one polymer with excellent mechanical properties and the other with high affinity with the electrolyte solution [6].

PEO polymer is most used as polymer electrolyte and P(VDF-TrFE)/PEO blend have been produced with a room temperature ionic conductivity of 0.25 mS cm^{-1} for 1M $LiClO_4.3H_2O$ electrolyte solution, despite the blends do not showed any porous microstructure [26].

The P(VDF-TrFE)/PEO polymer blend was tested for lithium-ion battery applications with an 1 M lithium hexafluorophosphate ($LiPF_6$) in ethylene carbonate/dimethyl carbonate (EC-DMC, 1/1 in weight) electrolyte solution and the capacity vs. current rate dependence of Li/Sn-C half- cells indicated reduced values in the blend membrane with respect to P(VDF-TrFE) ones due to the lower ion conductivity of the blends [27].

Thus, the objective of this work is to evaluate physical characteristics and battery performance of porous P(VDF-TrFE)/PEO polymer blends as a function of the porosity, by partially or totally removing PEO from the membranes.

2. Experimental Details

2.1. Materials

P(VDF-TrFE) (M_w = 350 000 g/mol) and PEO (M_w = 100 000 g/mol) were acquired from Solvay and Polysciences, respectively. The solvent N,N-dimethylformamide (DMF, 99.5%), Propylene carbonate (PC, anhydrous 99.0%) and Lithium Bis (Trifluoromethanesulfonyl) Imide (LiTFSI) were purchased from Aldrich.

2.2. Polymer Blend Preparation

The P(VDF-TrFE)/PEO blends were prepared with a composition of 50/50 weight ratio by dissolving the adequate amounts of both polymers in DMF at a 15/85 w/v polymer/solvent ratio. The choice of this composition is due to the fact that larger PEO contents in the polymer blend lead to very fragile membranes and removing PEO yields a discontinuous material [28, 29]. The polymers were dissolved at 60 ºC during 4 hours by stirring until a homogeneous and transparent solution was obtained. The solutions were deposited in Petri dishes and the solvent evaporated at 70 ºC for two hours. Finally, complete removal of the solvent was achieved in vacuum for another three hours at 70 ºC. Samples with average thickness of 300 μm were obtained.

2.3. Removal of PEO and Measurement of the Degree of Porosity

Porosity was obtained by removing PEO from the samples. Due to its hydrophilic nature, PEO was removed just by fully immersing the samples in water for different times.

The percentage of the removal of PEO was calculated after different immersion times using the following equation:

$$\%PEO\,removal = \left(\frac{W_0 - W_i}{W_0} \right) \times 100 \quad (1)$$

where W_0 and W_i denote the weight of dried membrane and weight of membrane after soaked in water, respectively.

The value of porosity created in the P(VDF-TrFE)/PEO blend membrane is proportional to the initial percentage of PEO less of the percentage of the PEO polymer remaining after PEO removal in each time.

2.4. Electrolyte Solution and Uptake

The electrolyte uptake was determined, after immersing the membranes in a solution of 1 M LiTFSI in PC for 24 hours, by equation 2:

$$\varepsilon = \left(\frac{M - M_0}{M_0} \right) \times 100\,\% \qquad (2)$$

where **ε** is the uptake of the electrolyte solution, M_0 is the mass of the membrane and M is the mass of the membrane after immersion in the electrolyte solution**.** This electrolyte solution exhibits similar viscosity as the 1 M $LiPF_6$-EC-DMC electrolyte commonly employed in lithium-ion batteries [30]. The electrical conductivity of the 1 M LiTFSI in PC electrolyte is $\sigma_0 = 6.5 \times 10^{-3}$ S cm^{-1} at 25 °C.

2.5. Characterization Techniques

The microstructure of the membranes was examined in a scanning electron microscope, Jeol JSM-5410 after deposition of a gold conductive layer of sputtered gold.

Contact angle measurements (sessile drop in dynamic mode) were performed at room temperature in a Data Physics OCA20 device using ultrapure water (3 mL droplets) as the test liquid. At least 3 measurements were carried out in each sample in different sample locations and the average contact angle was calculated.

The crystalline phase of each polymer within the blend was determined by Fourier transform infrared spectroscopy (FTIR) using a Thermo Nicoled Nexus equipment in ATR mode over a range of 650–1750 cm^{-1} with 64 scans at resolution of 4 cm^{-1}.

Differential scanning calorimetry analysis (DSC) was carried out with a Perkin-Elmer Pyris 1 DSC instrument under a flowing nitrogen atmosphere between 25 and 200 ^{o}C at a heating rate of 10 ^{o}C.min^{-1}. All samples were measured in 30 μL aluminium pans with perforated lids to allow the release and removal of decomposition products. The degree of crystallinity (ΔX_{cryst}) for each polymer was calculated using equation 3:

$$\Delta X_c = \frac{\Delta H_f}{\Delta H_{100}} \quad , \qquad (3)$$

where ΔH_f is the melting enthalpy of the sample and ΔH_{100} is the melting enthalpy for a 100% crystalline sample, being 103.4 J.g^{-1} for P(VDF-TrFE) [31] and 203 J.g^{-1} for PEO [32].

Dynamic mechanical analysis (DMA) was performed in a Seiko DMS210 apparatus in the tensile mode. The storage modulus and loss tangent were measured at room temperature as a function of frequency from 0.05 Hz to 20 Hz. Samples with typical dimensions of 10×4×0.030 mm were used.

2.5.1. Electrochemical Evaluation

The ionic conductivity was evaluated with an Autolab PGSTAT-12 (Eco Chemie) set-up for frequencies between 500 mHz and 65 kHz, using a constant volume support equipped with gold blocking electrodes located within a Büchi TO 50 oven. The sample temperature variation ranged from 20 to 140 ^{o}C and was measured by means of a type K thermocouple placed close to the films. The ionic conductivity was measured during the heating cycles and determined by

$$\sigma = \frac{t}{A \times R_b} \tag{4}$$

where t is the thickness, A is the area of the samples and R_b is the bulk resistance obtained from the intercept of the imaginary impedance (minimum value of Z'') with the slanted line in the real impedance (Z') through the Randles circuit [33]. The tortuosity (τ), the ratio between the effective capillarity to thickness of the sample, was determined by [34]:

$$\sigma_{eff} = \sigma_0 \frac{\phi}{\tau^2} \tag{5}$$

where σ_0 is the electrical conductivity of the liquid electrolyte, σ_{eff} is the conductivity of the membrane and the electrolyte set and ϕ is the porosity of the membrane.

The MacMullin number, N_M, describes the relative contribution of a separator to the cell resistance and is defined by [35]:

$$N_M = \frac{\sigma_0}{\sigma_{eff}} \tag{6}$$

where σ_{eff} is the conductivity of the membrane and liquid electrolyte pair and σ_0 is the conductivity of the pure liquid electrolyte

The evaluation of the electrochemical stability of the polymer blends was carried out within a dry argon-filled glovebox using a two-electrode cell configuration with a 25 μm diameter of gold microelectrode as working electrode and lithium disk counter electrode (10 mm diameter, 1mm thick, Aldrich, 99.9% purity) on a stainless steel

current collector. The sample was put between electrodes and the assembly was performed to an Autolab PGSTAT-12 (Eco Chemie) apparatus used to record voltammograms at a scan rate of 100 mVs^{-1}. Measurements were conducted at room temperature within a Faraday cage located inside the glovebox.

Li/C-$LiFePO_4$ half-cells were assembled in an argon-filled glove box (H_2O, O_2 < 1ppm) using Swagelok-type cells with 1.5 mm thick Li metal foil (7 mm diameter) as reference/counter electrode, a swollen P(VDF-TrFE)/PEO membrane (9 mm diameter) as separator, C-$LiFePO_4$ electrode (7 mm diameter) as working electrode and 1 M LiTFSI in a propylene carbonate (PC) as electrolyte. The C-$LiFePO_4$ cathode was prepared as described in [36].

The cycling performance of the Li/C-$LiFePO_4$ half-cells was carried out using a Biologic MPG station at room temperature. The galvanostatic cycling was performed within the 2.5-4.0 V voltage range, respectively, at low current rate (C5) and high current rate (2C). The rate capability was investigated at various discharge rates from C5 to 2C.

3.1. Results and Discussion

3.1.1. Morpholgy, Uptake, Porosity and Contact Angle

The membranes were immersed in water up to 7 days and the water was changed every day. The evolution of the PEO content in the samples is shown in figure 1: 89% of PEO was removed during the first day.

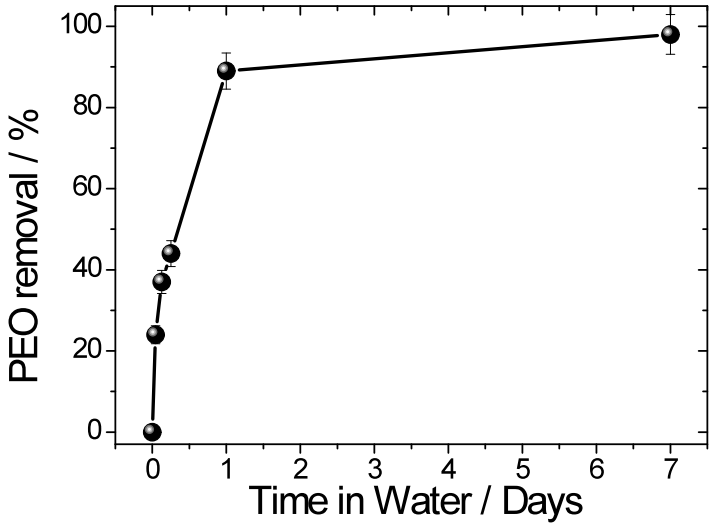

Figure 1 – PEO removal process in function of time

After removing the samples from the water, the drying process of the samples was performed in two steps: in open air for one day and in vacuum for another day. In the following, the samples will be named 0%, 25 % (1 hour), 38% (3 hours), 44% (6 hours), 90% (1 day) and 98% (7 days), respectively, representing the PEO removed from the membrane.

The surface and cross-section membrane morphology of the P(VDF-TrFE)/PEO blends are shown in figure 2 for samples with different PEO content.

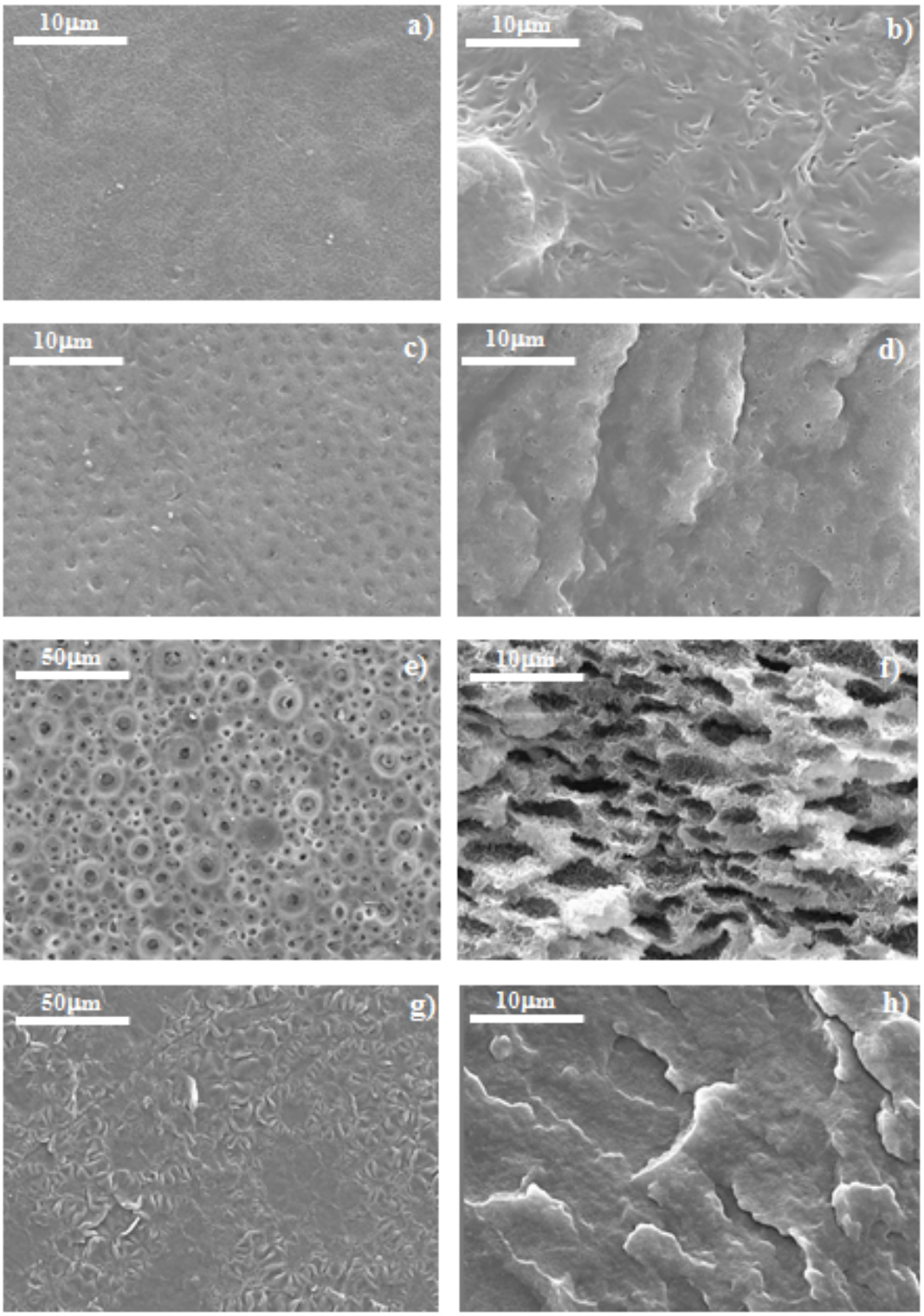

Figure 2 - Surface (left)and cross-section (right) SEM images respectively of the P(VDF-TrFE)/PEO blends with different percentage of PEO removal: a-b) 0%, c-d) 38%, e-f) 90% and g-h) 98%.

The figure 2 a) and b) show the surface and cross-section morphology of the P(VDF-TrFE)/PEO blend showing fibrilar structure characteristic of P(VDF-TrFE) attributed

to the lamellar structures of the all trans β crystalline phase [37]. Since melting temperature of PEO is lower that 70ºC, PEO crystallizes during cooling from 70ºC to room temperature, in this process, pure PEO would form large spherulites (> 50μm diameter, results not shown), which are not observed in figure 2a-b) [28] and indicating that the crystallization kinetics of PEO is hindered by the presence of P(VDF-TrFE). The variation of the microstructure of the blends after PEO elimination is shown in figure 2 c-f for two different percentage of removal: 38% and 89%, respectively.

Figure 2 shows that the pore structure (both porosity and pore size) increases with increasing PEO removal up to 90%. For PEO removal above 90%, the collapse of the pore structure is observed as shown figure 2 g-h for 98% PEO removal.

Thus formation of the pore structure is fully determined by the elimination of the PEO as well as the interconnectivity which increases with decreasing PEO content as shown in the cross-section SEM images (figure 2 d) and 2 f)). Figure 2 f) shows a highly porous structure able to absorb higher electrolyte contents in the three-dimensionally continuous channels in comparison to figure 2 d).

As previously reported, the conductivity of P(VDF-TrFE)/PEO based lithium salt complexes is in large extent determined by the continuity and ionic mobility in the PEO phase that depends on the electrolyte solution content in the porous membrane (uptake value) [26].

Figure 3 illustrates the uptake of the electrolyte solution for the different percentage of PEO removal as a function of the dipping time.

It has been shown for PVDF/PEO blends with 1M $LiClO_4$ in PC electrolyte solution, that the PEO content has large influence in both rate and ratio of liquid electrolyte uptake [38] Figure 3 shows uptake values of 123% for the polymer blend without elimination of PEO due to stronger interactions of the organic electrolyte (e.g., solvent molecules and lithium salt) with the PEO host compound associated with a plasticized structure [39].

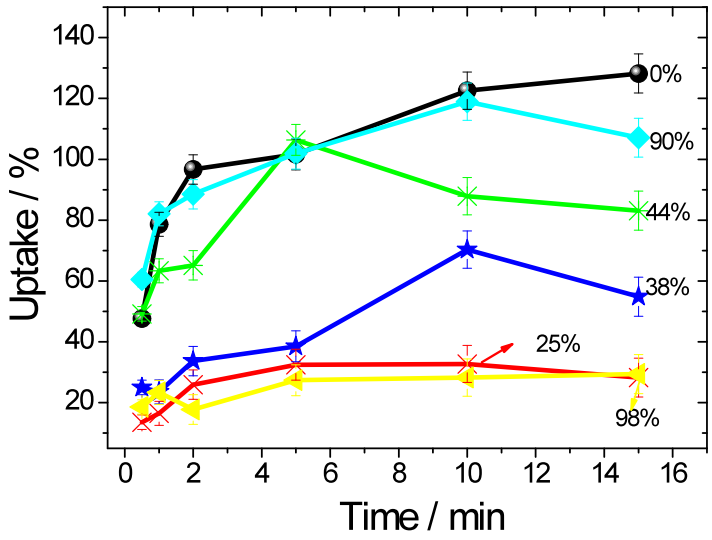

Figure 3 – Uptake value as a function of time for samples with different PEO content (indicated as PEO removal).

Independently of the PEO removal (figure 3), the blend membranes achieve saturation after approximately 10 min, with a 1M LiTFSI in PC content indicating that the void volume was fully filled. Liquid electrolyte uptake occurs in different stages: the electrolyte fill the pores (whenever present), then it swells into the amorphous phase and finally it is absorbed into the P(VDF-TrFE).

The uptake value depends on the percentage of PEO removal in the P(VDF-TrFE)/PEO blend as shown in the figure 4. For the porous membranes of P(VDF-TrFE)/PEO blend, the uptake value after 10 minutes are 28%, 55%, 83% and 107% for 25%, 38%, 44% and 90% of PEO removal, respectively. Comparing the samples with PEO polymer elimination, it is observed that they present enhanced ability to absorb and retain the electrolyte solution except for sample with 98% of PEO removal due to the collapse of the microstructure (figure 2 g-h). The large uptake of P(VDF-TrFE)/PEO blend without PEO removal is due to stronger interactions of the organic electrolyte through the plasticizer effect [40].

This process depends thus on PEO content, porosity and pore connectivity (figure 4 and figure 2 (microstructure images)).

Figure 4 shows the maximum uptake value after 15 min in electrolyte solution as well as the porosity as a function of PEO removal in the P(VDF-TrFE)/PEO blends.

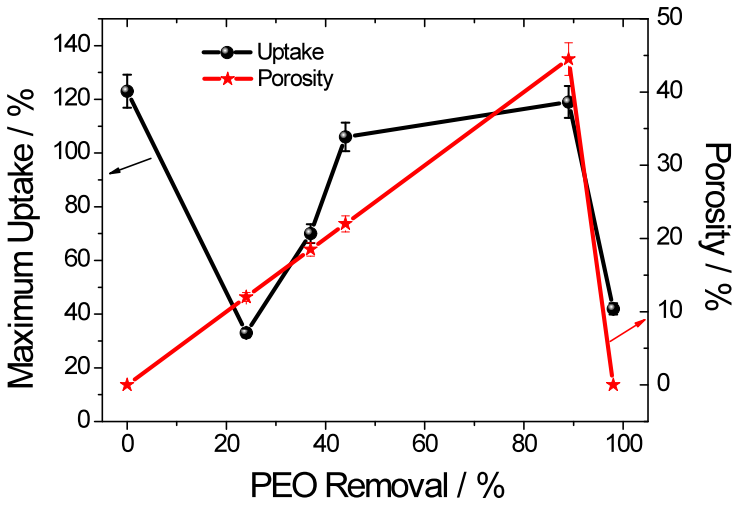

Figure 4 – Uptake value and degree of porosity as a function of the percentage of PEO removal.

Taking into account figure 4, the porosity of the polymer blend increases from 12% to 44.5%, which in turn increases the uptake of liquid electrolyte from 33% to 119% with the elimination of PEO polymer. The fast uptake process can be attributed to the porosity, fully interconnected open pore structure and good affinity to the electrolyte.

The uptake value increases with increase of the porosity for the membranes with PEO removal which in turn will affect the ionic conductivity of the membranes (figure 9 and 10) due to the liquid trapped also in the pores [41]. In addition to the pores, the liquid electrolyte are also absorbed in the amorphous matrix of the P(VDF-TrFE) polymer, which causes swelling.

The hydrophilic or hydrophobic behavior of the polymer blends is another important parameter to be considered in the development of battery separator applications as it reflects adhesion of the porous membrane with electrodes and it can be assessed through the measurement of the contact angle, i.e, wettability. Good wettability also allows the separator to better retain the electrolyte solution, thereby facilitating fast ion transport between the two electrodes during charge and discharge cycling [42].

The contact angle as a function of the percentage of PEO removal is illustrated in the figure 5.

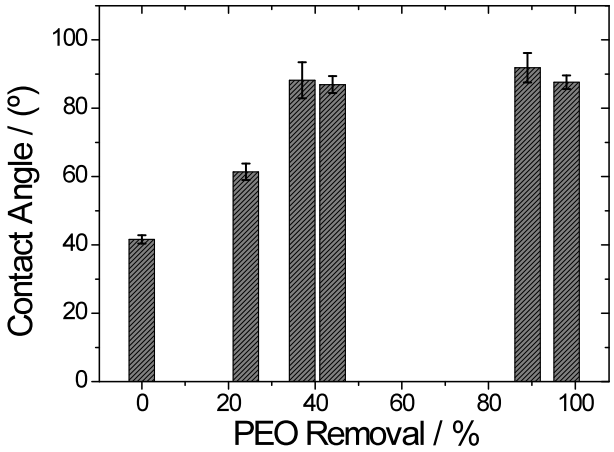

Figure 5 – Contact angle of the P(VDF-TrFE)/PEO blend as a function of percentage of PEO removal.

The low contact angle (~40º) observed for the membrane without elimination of PEO is due to the hydrophilic nature of PEO. Further, the contact angle increases with increasing PEO removal (figure 5) –i.e. decreasing PEO content- due to the morphology variations of porous membranes but, in particular, due to the larger relative content of hydrophobic P(VDF-TrFE). The maximum value of the contact angle (~92º) is observed for 90% of PEO removal.

3.1.2. FTIR, Thermal and Mechanical Results

The vibrational spectra of the P(VDF-TrFE)/PEO blend membranes was determined by FTIR spectroscopy as presented in figure 6. The assignment of the absorption bands for each polymer (P(VDF-TrFE) and PEO can be found in [28].

It was observed main absorption bands at 851 and 886 cm^{-1} corresponding to the all-trans conformation of the P(VDF-TrFE) polymer [43, 44]. In this way, the presence of PEO does not cause any relevant modification in crystal phase of P(VDF-TrFE).

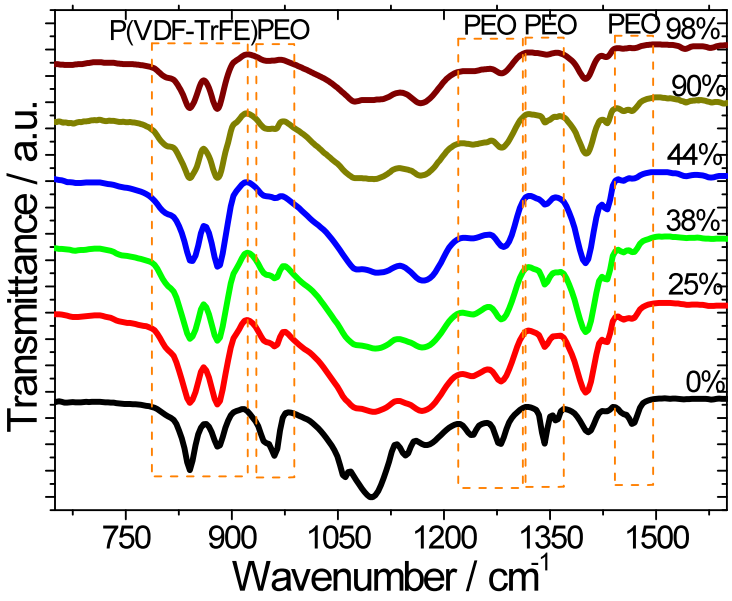

Figure 6 – FTIR spectra of the P(VDF-TrFE)/PEO blends as a function of percentage of PEO removal.

The absorption peaks of PEO are observed at 964, 1235-1280, 1343 and 1468 cm^{-1} that corresponds to CH_2 rocking, CH_2 twisting, CH_2 wagging and CH_2 scissoring [28]. Figure 6 shows that, as expected, the absorption peaks of PEO decrease with increasing the percentage of PEO removal.

The safety of lithium ion batteries is a critical parameter strongly dependent on the thermal stability of the separators. The thermal stability in the membranes has been determined by the melting temperature, from which also the degree of crystallinity has been calculated.

The DSC heating scans of the different P(VDF-TrFE)/PEO blends is shown in figure 7.

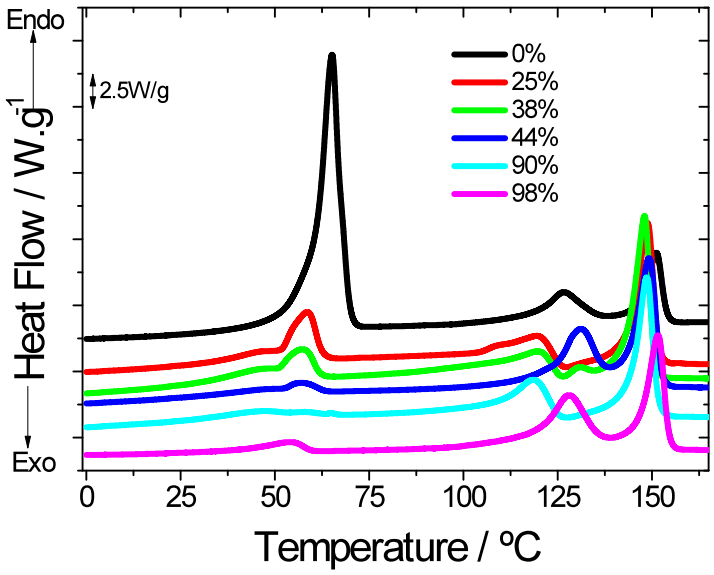

Figure 7 – DSC thermograms of the P(VDF-TrFE)/PEO blends as a function of percentage of PEO removal

Figure 7 shows three endothermic peaks for all membranes. The lower temperature peak appears around 56-66ºC and corresponds to the melting temperature of PEO, and therefore decreases with increasing of percentage of PEO removal, i.e, with decreasing PEO content [45]. The other higher temperature endothermic peaks correspond to the P(VDF-TrFE) polymer: the one at ~119 ºC corresponds to the ferroelectric (FE)–paraelectric (PE) transition (Curie transition) and the one around ~148 ºC corresponds to the melting temperature of the PE phase [46]. Melting temperatures and crystalline fraction calculated by applying Eq. 3 are shown in Table 1 as a function of PEO removal.

Table 1 – Degree of crystallinity and melting temperature for the different membranes as a function of the different percentage of PEO removal.

	P(VDF-TrFE)		PEO	
% PEO removal	Tf ± 3 (ºC)	χ ± 2 (%)	Tf ± 3 (ºC)	χ ± 2 (%)
0	148	35	66	70
25%	149	34	59	26
38%	148	36	57	18
44%	149	35	57	9
90%	151	33	56	1.7
98%	148	35	---	---

Ojo con los cálculos de la cristalinidad, tiene que tomarse como referencia la masa de PEO que queda en la muestra después de la extracción, los números que pones para que se ha dividido por la masa total de la muestra

Lo mismo para la cristalinindad del P(VDF-TrFE), hay que referirlo a su masa en la muestra

Table 1 shows that the degree of crystallinity and melting temperature of the P(VDF-TrFE) polymer is independent of the PEO removal. In relation to the degree of the crystallinity of PEO, it is observed that decreases with increasing of percentage of PEO removal, i.e. with decreasing PEO content due to a destruction of the crystalline regions at the amorphous/crystalline interfaces [47]. For PEO, increasing the amorphous content is beneficial for achieving a higher ionic conductivity [48].

The determination of the mechanical properties for the polymer blends is fundamental for this application. The mechanical properties of the samples were obtained by dynamical mechanical analysis (DMA) at room temperature through the measurements of the storage modulus *E´* (figure 8).

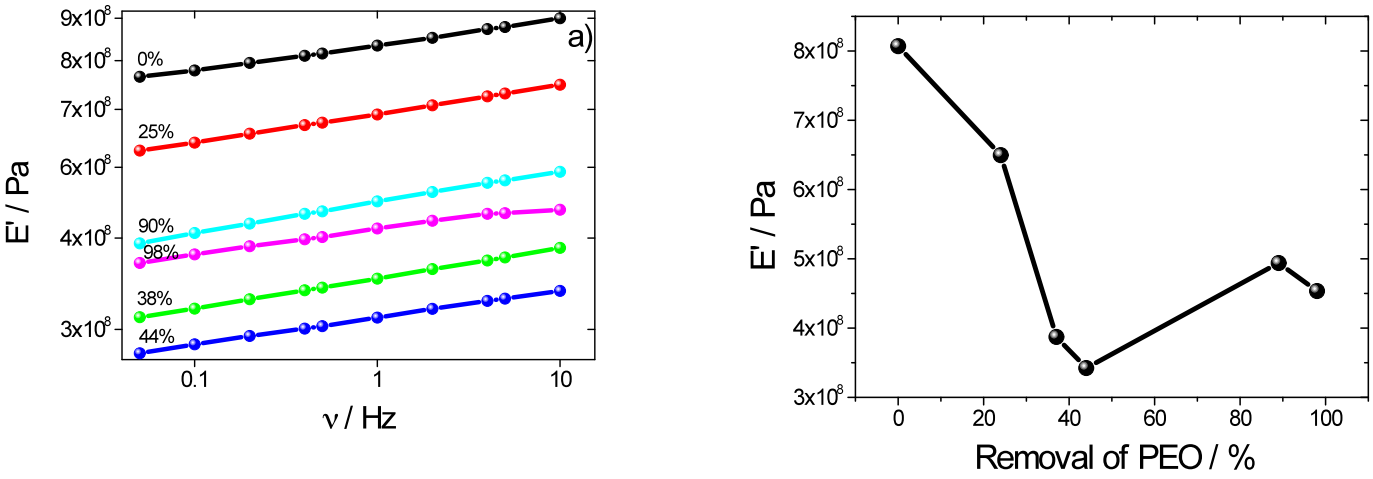

Figure 8 – DMA curves for (a): storage modulus, E´ vs log (ν) for all P(VDF-TrFE)/PEO blends and (b): storage modulus, E´ as a function of the percentage of PEO removal at 1Hz.

It is shown that an increase in E´ (figure 8a) is detected for all polymer blends with increasing frequency in the analyzed range from 0.05 to 10 Hz, which is attributed to the slow time response of these viscoelastic polymers at room temperature, far from the glass transition temperature (above in the case of PEO, and below in the case of P(VDF-

TrFE)) [49]. The elastic modulus (E´) is also strongly dependent (figure 8a and b) on the membrane microstructure.

Figure 8b shows that elastic modulus (E´) decreases with increasing of the degree of porosity (proportional to percentage of PEO removal) except for samples with high pore size (figure 2f) where the collapse of the structure also occurs (figure 2g).

3.1.3. Ionic Conductivity and Electrochemical Stability

Figure 9 represents the Nyquist curves of the liquid electrolyte soaked in all P(VDF-TrFE)/PEO blends determined by AC impedance at 50ºC. For all samples, independently of the frequency, a linear dependence is observed. This behavior represents the diffusion of the polymer chain with coordinated ions and the liquid uptake of the polymeric blend membrane that benefits ion migration which results in a low impedance.

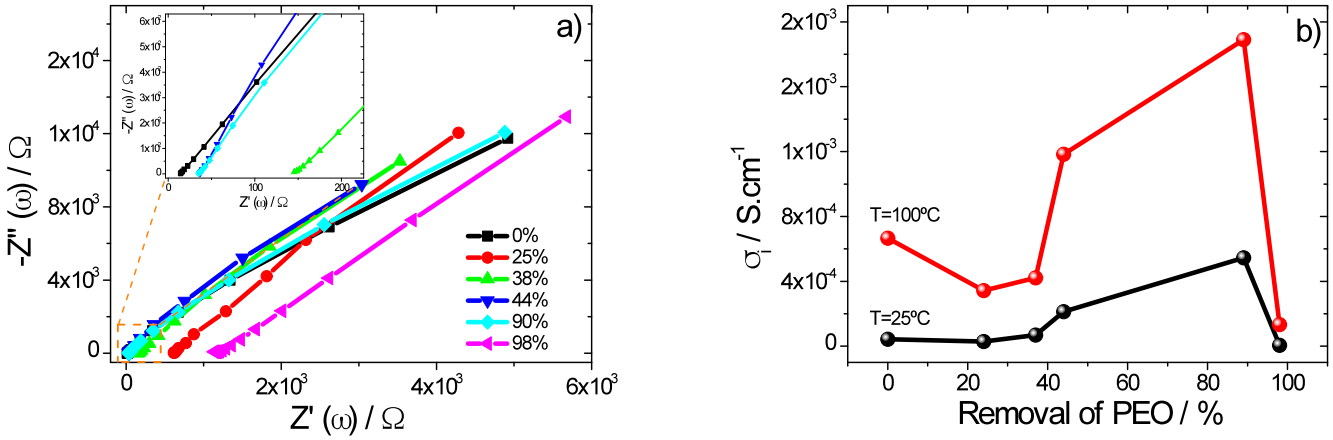

Figure 9 - (a) Nyquist plots at 50 ºC and (d) ionic conductivity at 25 ºC and 100 ºC for the different P(VDF-TrFE)/PEO blends.

It is observed that the ionic conductivity (σ_i), determined by Eq. (4), increases with increasing the percentage of PEO removal (i.e. decreasing PEO content), as shown in figure 9b, independently of the measured temperature. Increasing temperature leads, on the other hand, to an overall increase of the conductivity.

For the P(VDF-TrFE)/PEO blends, the highest room temperature ionic conductivity was 0.54 mS cm^{-1} for PEO removal of 90% as shown in table 2.

This shows that the highest ionic conductivity is obtained for the polymer blends with the highest electrolyte uptake (table 2). The liquid electrolyte uptake depends on the porosity which in turn affects ionic conductivity. It is shown that higher porosity leads to higher electrolyte uptake which results in higher ionic conductivity (figure 4 and 9, table 2).

Table 2 – Effective degree of porosity, room temperature ionic conductivity, tortuosity, MacMullin number (N_M) and activation energy (E_a) of the different polymer blend separator membranes soaked in 1M LiTFSI-PC.

	% PEO removal					
Property	**0%**	**25%**	**38%**	**44%**	**90%**	**98%**
Effective porosity ϕ_{eff} / %	0	12	18.5	22	44.5	0
σ_i at 25ºC / mS.cm^{-1}	0.04	0.03	0.07	0.21	0.54	0.01
N_M	163	217	93	31	12	650
τ_{eff}	0	5	4	3	2	0
E_a / $kJmol^{-1}$	8.7	13.4	9.1	8.1	6.3	12.6

Table 2 shows, together with the ionic conductivity and degree of porosity, the tortuosity value and the MacMullin number (N_M) calculated by Eqs. 5 and 6, respectively.

It is observed that the ionic conductivity follows the same trend as the porosity, which in turn depends on the percentage of PEO removal.

The tortuosity describes a conductivity pathway through straight channels of uniform orientation parallel to the transport direction. Typically, $\tau_{eff} > 1$ as $\tau_{eff} = 1$ describes an ideal porous body with cylindrical and parallel pores. The value of tortuosity of the membranes is between 2 and 5 depending on the porosity and reveals that a major contribution for the conduction process is the swelling of the amorphous phase of P(VDF-TrFE). A low tortuosity value is observed for the sample with PEO removal of 90%, which supports better pore connectivity (figure 2f) [50].

It is also observed that the MacMullin number (N_M) depends on the PEO removal, being also correlated with the tortuosity and the affinity between the membrane and the electrolyte solution [51]. The lowest value of the MacMullin number was obtained for

P(VDF-TrFE)/PEO polymer blend with PEO removal of 90%, that blend presenting a high degree of porosity, high electrolyte uptake and low tortuosity.

Figure 10 shows the ionic conductivity as a function of temperature. The log σ vs $1000T^{-1}$ shows a linear correlation in the temperature range between 25ºC and 100ºC, indicating that the temperature dependence of the ionic conductivity obeys the Arrhenius model: $\sigma = \sigma_0 \exp\left[-E_a/RT\right]$ where R is the gas constant, σ_0 the pre-exponential factor and T the testing temperature.

The activation energy for ion transportation within the polymer blends is listed in Table 2. It is shown that E_a depends on PEO removal and its behavior is proportional to the ionic conductivity value and liquid electrolyte uptake.

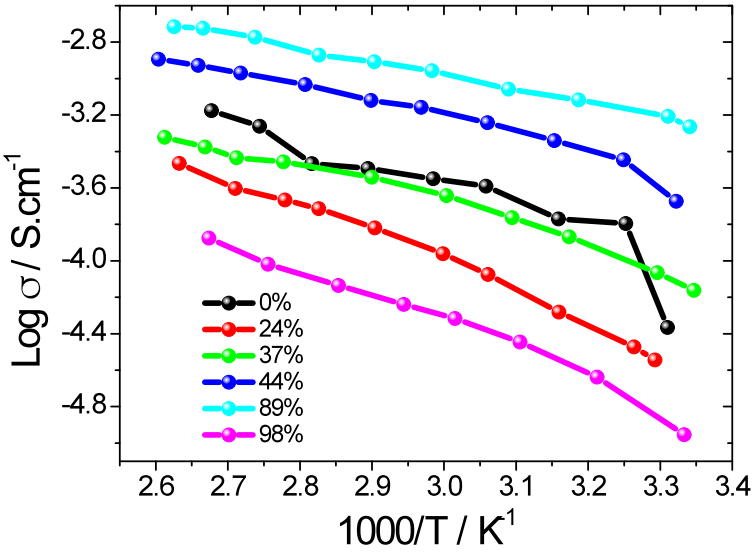

Figure 10 - Log σ as a function of 1000/T for the different polymer blend samples.

Figure 10 shows that the ionic conductivity increases with increasing temperature due to the increase of the free volume [52] and segmental mobility of the polymer with increasing temperature, as well as with the larger concentration of ionic charge carriers and their mobility [53]. The ionic conductivity behavior do not exhibit a clear change around the melting point of PEO for any sample since the ionic motion is expected to be coupled to local modes of the P(VDF-TrFE) chains.

For battery system applications it is necessary to determine the electrochemical stability of the separators. Linear sweep voltammetry curves of Li/polymer blend/gold electrode cell at 25ºC are shown in figure 11.

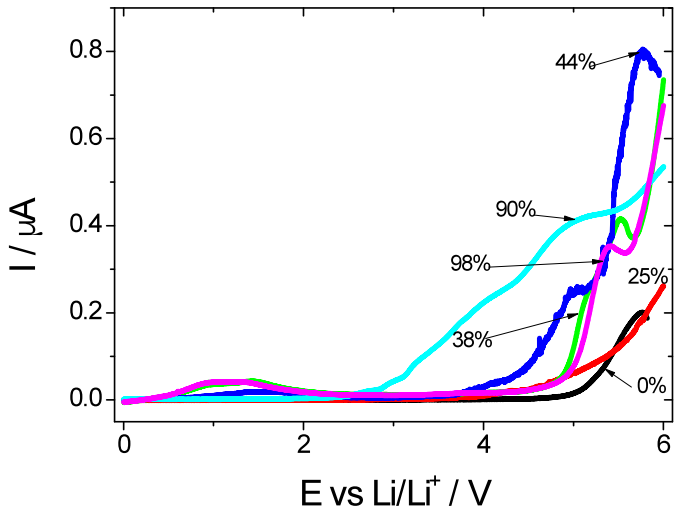

Figure 11 – Voltammogram at a 0.5 V/s scanning rate, for the polymer blend samples.

In the figure 11 it is observed a rapid increase in current around 5V (vs. Li^+/Li) , associated with the oxidative decomposition of the liquid electrolyte [54] but the current values are very small and could be considerate as a parasitic current that not affect the electrochemical window stability of these samples up to 5V. In this way, this effect is independent of the PEO removal. Thus, the overall results show that PEO removal improves the degree of porosity, ionic conductivity and does not affect the electrochemical stability of the P(VDF-TrFE)/PEO polymer blend, showing suitable properties for lithium-ion battery applications.

3.1.4. Battery performance evaluation in Li/C-LiFePO$_4$ Swagelok cell

Li/C-LiFePO$_4$ Swagelok cells using P(VDF-TrFE)/PEO polymer blends with 0%, 44% and 90% of PEO removal as separators were evaluated between 2.5V and 4.0V at 25ºC to demonstrate the applicability of the materials in lithium-ion battery applications.

Figure 12 a) and b) presents the 10th charge-discharge curves at C5 and 2C, respectively. No unstable voltage profiles were observed for any of the cells. In figure 12a at C5, it is found that the cells deliver discharge capacities of 124, 82 and 63 mAhg^{-1} when the P(VDF-TrFE)/PEO polymer blend with PEO removal values of 90%, 44% and 0% are used as separators, respectively. For 2C rate, the discharge capacities values are 47, 21 and 10 mAhg^{-1} for PEO removal of 90%, 44% and 0%, respectively (figure 12b). Independently of the scan rate (figure 12 a and b), the discharge capacity increases with increasing PEO removal in the P(VDF-TrFE)/PEO polymer blend. Thus, independently of the scan rate, the discharge capacity of the cells with polymer blend electrolyte follows the order 90% > 44% > 0%. This behavior is related to the ionic conductivity value, higher ionic conductivity leading to improved repeated intercalation/de-intercalation of Li^+ in/from the electrode materials [54].

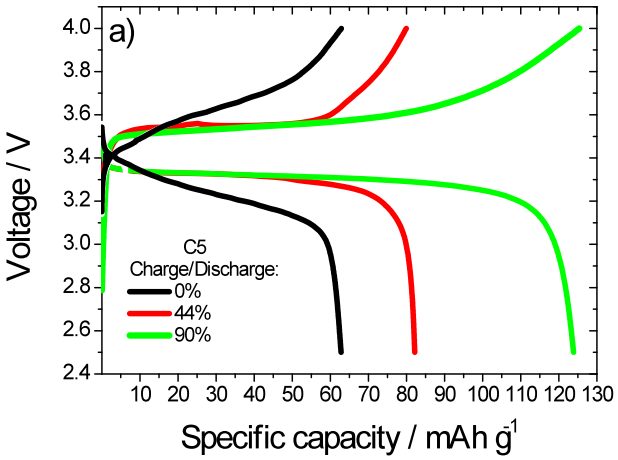

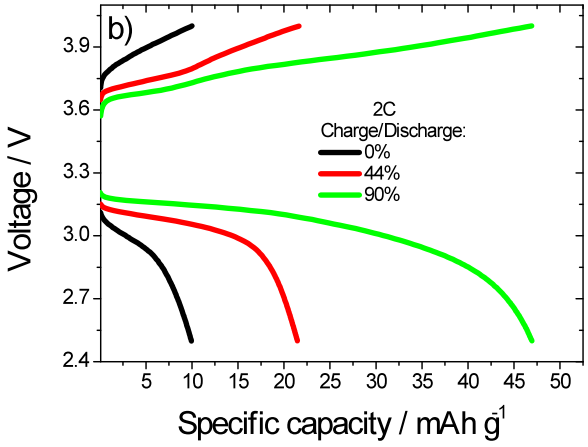

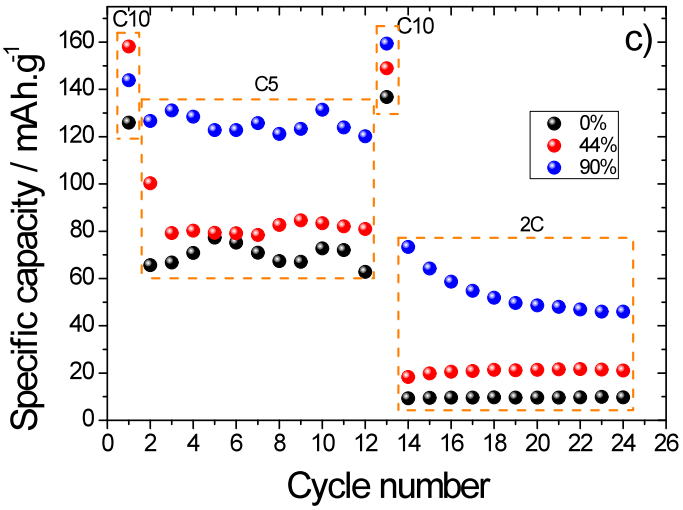

Figure 12 – Charge-discharge curves for Li/C-$LiFePO_4$ at: a) C5 and b) 2C. c) Discharge capacity as a function of cycle number.

The discharge capacities as a function of cycle number for two scan rate (low rate, C5 and medium rate, 2C) are shown in figure 12c). Independently of the scan rate, the discharge capacity is stable as a function of the cycle number. In relation to the 2C scan rate for PEO removal of 90%, the discharge capacity slightly decreases with increasing the cycle number due to interfacial resistance between electrode and separator membrane [55]. The delivered capacity at 2C shows a low value in comparison to C5 due to the polarization associated with the electrolyte diffusion kinetics [27].

It is observed that all the cells show relatively stable performance for both scan rates in the cycling number range under consideration.

Delivered capacity and capacity retention (capacity normalized with respect to the nominal one) as a function of current rate dependence of the polymer blend with high ionic conductivity (90% PEO removal) is shown in the figure 13. A progressive, almost linear, decrease in capacity is observed with increasing current density up to 1 C, associated to the diffusion phenomena taking place within the electrode active material phase and polymer electrolyte separator membrane [56].

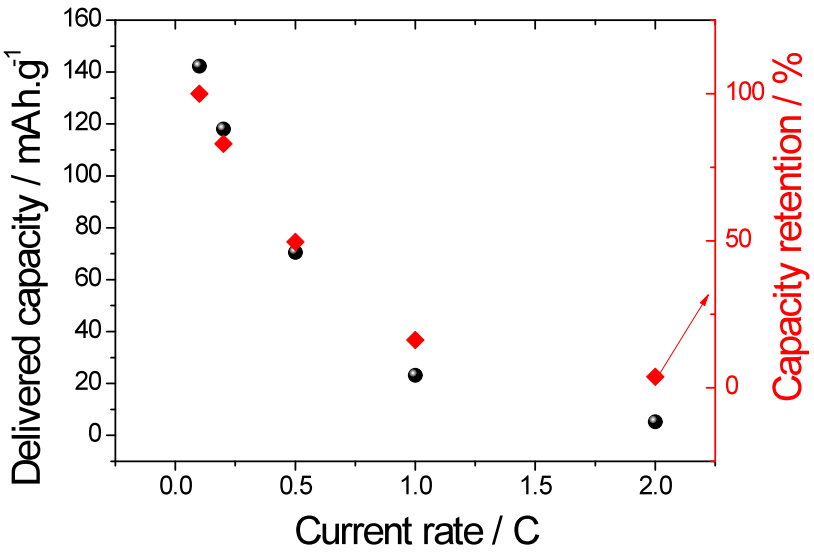

Figure 13 - Delivered capacity and capacity retention vs. current rate dependence

Figure 13 shows that above 1C a very contained decay in the delivered capacity and capacity retention is observed due to the intercalation of the Li^+ ion present in the electrode film and to Ohmic polarization [57].

These results illustrate for this polymer blend system that polymer blend with 90% PEO removal shows the best performance as lithium ion battery separator and could be used for battery application. On the other hand, if we compare its performance with that of highly porous pure P(VDF-TrFE) membrane reported in reference [58] (porosity, 72% and uptake, 396%, 0.32 mS/cm ionic conductivity), it can be concluded that ionic conductivity value depends not only of degree of porosity but also of the interaction between polymer and electrolyte solution. The ionic conductivity value affects the performance of separator in lithium-ion battery application in that this P(VDF-TrFE)/PEO system in function of PEO removal is very promissing for this application.

Conclusions

The effect of the removal of poly(ethylene oxide) in the polymer blends based on poly(vinylidene fluoride-trifluoroethylene)/poly(ethylene oxide) has been investigated for Li-ion battery separator applications. The pristine polymer blend membranes were prepared by solvent casting at 70ºC. The (partial to total) elimination of PEO produces interconnected micropores in the polymer blends influencing the electrolyte uptake value of 1M LiTFSI in PC.

The IR vibration modes characteristic of P(VDF-TrFE) are not influenced by the elimination of PEO in the polymer blend. The mechanical properties depend on the PEO removal and correlates with the degree of crystalinity.

Electrical properties of the polymer blend membranes are influenced by PEO removal and are dominated by diffusion, the ionic conductivity as a function of temperature following the Arrhenius behavior. The ionic conductivity has a maximum for the samples with 90% of PEO removal e, reaching a value of 0.54 $mS.cm^{-1}$ at room temperature.

P(VDF-TrFE)/PEO polymer blend with 90% PEO removal exhibit excellent cycling performance, i.e, 124 $mAhg^{-1}$ at C5 and 47 $mAhg^{-1}$ at 2C in comparison with other samples. Also presents good electrochemical stability and could be applied as promising separator for applications in lithium-ion batteries.

Acknowledgements

This work is funded by FEDER funds through the "Programa Operacional Factores de Competitividade–COMPETE" and by national funds from FCT–Fundação para a Ciência e a Tecnologia, in the framework of the strategic project Strategic Projects PEST-C/FIS/UI607/2011 and grants SFRH/BD/68499/2010 (C.M.C.), SFRH/BD/90313/2012 (A.G.) and SFRH/BD/66930/2009 (J.N.P.). The authors thank funding from Matepro–Optimizing Materialsand Processes", ref. NORTE-07-0124-FEDER-000037", co-funded by the "Programa Operacional Regional do Norte" (ON.2–O Novo Norte), under the "Quadro de Referência Estratégico Nacional"(QREN), through the "Fundo Europeu de Desenvolvimento Regional" (FEDER).

JLGR acknowledges the support of the Ministerio de Economía y Competitividad, MINECO, through the MAT2013-46467-C4-1-R project (including FEDER finantial support). CIBER-BBN is an initiative funded by the VI National R&D&i Plan 2008–

2011, Iniciativa Ingenio 2010, Consolider Program, CIBER Actions and financed by the Instituto de Salud Carlos III with assistance from the European Regional Development Fund.

References

1. Yoshio, M., R.J. Brodd, and A. Kozawa, *Lithium-Ion Batteries: Science and Technologies*2010: Springer.
2. Tarascon, J.M. and M. Armand, *Issues and challenges facing rechargeable lithium batteries.* Nature, 2001. **414**(6861): p. 359-367.
3. Wright, P.V., *Developments in Polymer Electrolytes for Lithium Batteries.* MRS Bulletin, 2002. **27**(08): p. 597-602.
4. Meyer, W.H., *Polymer Electrolytes for Lithium-Ion Batteries.* Advanced Materials, 1998. **10**(6): p. 439-448.
5. Scrosati, B. and J. Garche, *Lithium batteries: Status, prospects and future.* Journal of Power Sources, 2010. **195**(9): p. 2419-2430.
6. Di Noto, V., et al., *Polymer electrolytes: Present, past and future.* Electrochimica Acta, 2011. **57**(0): p. 4-13.
7. Wright, P.V., *Polymer electrolytes—the early days.* Electrochimica Acta, 1998. **43**(10–11): p. 1137-1143.
8. Agrawal, R.C. and G.P. Pandey, *Solid polymer electrolytes: materials designing and all-solid-state battery applications: an overview.* Journal of Physics D: Applied Physics, 2008. **41**(22): p. 223001.
9. Thakur, V.K., et al., *Hybrid Materials and Polymer Electrolytes for Electrochromic Device Applications (Adv. Mater. 30/2012).* Advanced Materials, 2012. **24**(30): p. 4070-4070.
10. Zhou, D., et al., *Non-Volatile Polymer Electrolyte Based on Poly(propylene carbonate), Ionic Liquid, and Lithium Perchlorate for Electrochromic Devices.* The Journal of Physical Chemistry B, 2013. **117**(25): p. 7783-7789.
11. Barbosa, P.C., et al., *Solid-state electrochromic devices using pTMC/PEO blends as polymer electrolytes.* Electrochimica Acta, 2010. **55**(4): p. 1495-1502.
12. Wang, Y., et al., *A review of polymer electrolyte membrane fuel cells: Technology, applications, and needs on fundamental research.* Applied Energy, 2011. **88**(4): p. 981-1007.
13. Li, Q., et al., *Approaches and Recent Development of Polymer Electrolyte Membranes for Fuel Cells Operating above 100 °C.* Chemistry of Materials, 2003. **15**(26): p. 4896-4915.
14. Opekar, F. and K. Štulík, *Electrochemical sensors with solid polymer electrolytes.* Analytica Chimica Acta, 1999. **385**(1–3): p. 151-162.
15. Latham, R.J., S.E. Rowlands, and W.S. Schlindwein, *Supercapacitors using polymer electrolytes based on poly(urethane).* Solid State Ionics, 2002. **147**(3–4): p. 243-248.
16. Costa, C.M., M.M. Silva, and S. Lanceros-Mendez, *Battery separators based on vinylidene fluoride (VDF) polymers and copolymers for lithium ion battery applications.* RSC Advances, 2013. **3**(29): p. 11404-11417.

17. Song, J.Y., Y.Y. Wang, and C.C. Wan, *Review of gel-type polymer electrolytes for lithium-ion batteries.* Journal of Power Sources, 1999. **77**(2): p. 183-197.
18. Nunes-Pereira, J., C.M. Costa, and S. Lanceros-Méndez, *Polymer composites and blends for battery separators: State of the art, challenges and future trends.* Journal of Power Sources, 2015. **281**(0): p. 378-398.
19. Popall, M., et al., *ORMOCERs as inorganic–organic electrolytes for new solid state lithium batteries and supercapacitors.* Electrochimica Acta, 1998. **43**(10–11): p. 1155-1161.
20. Murata, K., *An overview of the research and development of solid polymer electrolyte batteries.* Electrochimica Acta, 1995. **40**(13–14): p. 2177-2184.
21. Arora, P. and Z. Zhang, *Battery Separators.* Chemical Reviews, 2004. **104**(10): p. 4419-4462.
22. Karan, N.K., et al., *Solid polymer electrolytes based on polyethylene oxide and lithium trifluoro- methane sulfonate (PEO–LiCF3SO3): Ionic conductivity and dielectric relaxation.* Solid State Ionics, 2008. **179**(19–20): p. 689-696.
23. Chun-Guey, W., et al., *New solid polymer electrolytes based on PEO/PAN hybrids.* Journal of Applied Polymer Science, 2006. **99**(4): p. 1530-1540.
24. Costa, C.M., et al., *Influence of processing parameters on the polymer phase, microstructure and macroscopic properties of poly(vinilidene fluoride)/Pb(Zr0.53Ti0.47)O3 composites.* Journal of Non-Crystalline Solids, 2010. **356**(41–42): p. 2127-2133.
25. Costa, C.M., et al., *Effect of degree of porosity on the properties of poly(vinylidene fluoride–trifluorethylene) for Li-ion battery separators.* Journal of Membrane Science, 2012. **407–408**(0): p. 193-201.
26. Costa, C.M., et al., *Novel poly(vinylidene fluoride-trifluoroethylene)/poly(ethylene oxide) blends for battery separators in lithium-ion applications.* Electrochimica Acta, 2013. **88**(0): p. 473-476.
27. Costa, C.M., et al., *Poly(vinylidene fluoride)-based, co-polymer separator electrolyte membranes for lithium-ion battery systems.* Journal of Power Sources, 2014. **245**(0): p. 779-786.
28. Costa, C.M., et al., *Composition-dependent physical properties of poly[(vinylidene fluoride)-co-trifluoroethylene]–poly(ethylene oxide) blends.* Journal of Materials Science, 2013. **48**(9): p. 3494-3504.
29. Correia, D.M., et al., *Physicochemical properties of poly(vinylidene fluoride-trifluoroethylene)/poly(ethylene oxide) blend membranes for lithium ion battery applications: Influence of poly(ethylene oxide) molecular weight.* Solid State Ionics, 2014. **268, Part A**(0): p. 54-67.
30. Lee, S.-I., et al., *A study of electrochemical kinetics of lithium ion in organic electrolytes.* Korean Journal of Chemical Engineering, 2002. **19**(4): p. 638-644.
31. Sencadas, V., S. Lanceros-Méndez, and J.F. Mano, *Characterization of poled and non-poled β-PVDF films using thermal analysis techniques.* Thermochimica Acta, 2004. **424**(1–2): p. 201-207.
32. Porter, R.S., *Macromolecular physics, volume 3—crystal melting, Bernhard Wunderlich, Academic Press, New York, 1980, 363 pp. Price: $42.50.* Journal of Polymer Science: Polymer Letters Edition, 1980. **18**(12): p. 824-824.
33. Fernández-Sánchez, C., C.J. McNeil, and K. Rawson, *Electrochemical impedance spectroscopy studies of polymer degradation: application to biosensor development.* TrAC Trends in Analytical Chemistry, 2005. **24**(1): p. 37-48.

34. Karabelli, D., et al., *Poly(vinylidene fluoride)-based macroporous separators for supercapacitors.* Electrochimica Acta, 2011. **57**(0): p. 98-103.
35. Patel, K.K., J.M. Paulsen, and J. Desilvestro, *Numerical simulation of porous networks in relation to battery electrodes and separators.* Journal of Power Sources, 2003. **122**(2): p. 144-152.
36. Gören, A., et al., *Effect of drying temperature on poly(vinylidene fluoride) polymer binder for C-LiFePO4 cathode slurry preparation.* Electrochimica Acta, 2015. **Submitted**.
37. California, A., et al., *Tailoring porous structure of ferroelectric poly(vinylidene fluoride-trifluoroethylene) by controlling solvent/polymer ratio and solvent evaporation rate.* European Polymer Journal, 2011. **47**(12): p. 2442-2450.
38. Xi, J., et al., *PVDF–PEO blends based microporous polymer electrolyte: Effect of PEO on pore configurations and ionic conductivity.* Journal of Power Sources, 2006. **157**(1): p. 501-506.
39. Hassoun, J., et al., *A lithium ion battery using nanostructured Sn–C anode, LiFePO4 cathode and polyethylene oxide-based electrolyte.* Solid State Ionics, 2011. **202**(1): p. 36-39.
40. Suthanthiraraj, S.A. and M.K. Vadivel, *Effect of propylene carbonate as a plasticizer on (PEO)50AgCF3SO3:SnO2 nanocomposite polymer electrolyte.* Applied Nanoscience, 2012. **2**(3): p. 239-246.
41. Huang, H. and S.L. Wunder, *Ionic Conductivity of Microporous PVDF-HFP/PS Polymer Blends.* Journal of The Electrochemical Society, 2001. **148**(3): p. A279-A283.
42. Shin, W.-K., J.-H. Yoo, and D.-W. Kim, *Surface-modified separators prepared with conductive polymer and aluminum fluoride for lithium-ion batteries.* Journal of Power Sources, 2015. **279**(0): p. 737-744.
43. Martins, P., A.C. Lopes, and S. Lanceros-Mendez, *Electroactive phases of poly(vinylidene fluoride): Determination, processing and applications.* Progress in Polymer Science, 2014. **39**(4): p. 683-706.
44. Faria, L.O. and R.L. Moreira, *Infrared spectroscopic investigation of chain conformations and interactions in P(VDF-TrFE)/PMMA blends.* Journal of Polymer Science Part B: Polymer Physics, 2000. **38**(1): p. 34-40.
45. Afifi-Effat, A.M. and J.N. Hay, *Enthalpy and entropy of fusion and the equilibrium melting point of polyethylene oxide.* Journal of the Chemical Society, Faraday Transactions 2: Molecular and Chemical Physics, 1972. **68**(0): p. 656-661.
46. Hahm, S.-W. and D.-Y. Khang, *Crystallization and microstructure-dependent elastic moduli of ferroelectric P(VDF-TrFE) thin films.* Soft Matter, 2010. **6**(22): p. 5802-5806.
47. Marsac, P.J., P.U. Industrial, and P. Pharmacy, *Formation and Stabilization of Amorphous Molecular Level Solid Dispersions*2007: Purdue University.
48. Raghavan, P., et al., *Electrochemical performance of electrospun poly(vinylidene fluoride-co-hexafluoropropylene)-based nanocomposite polymer electrolytes incorporating ceramic fillers and room temperature ionic liquid.* Electrochimica Acta, 2010. **55**(4): p. 1347-1354.
49. Paul, S.A., et al., *Dynamic mechanical analysis of novel composites from commingled polypropylene fiber and banana fiber.* Polymer Engineering & Science, 2010. **50**(2): p. 384-395.

50. Quartarone, E., P. Mustarelli, and A. Magistris, *Transport Properties of Porous PVDF Membranes.* The Journal of Physical Chemistry B, 2002. **106**(42): p. 10828-10833.
51. Djian, D., et al., *Macroporous poly(vinylidene fluoride) membrane as a separator for lithium-ion batteries with high charge rate capacity.* Journal of Power Sources, 2009. **187**(2): p. 575-580.
52. Gray, F.M. and R.S.o. Chemistry, *Polymer electrolytes*1997: Royal Society of Chemistry.
53. Ren, T., et al., *Synthesis and characterization of novel crosslinked polyurethane–acrylate electrolyte.* Journal of Applied Polymer Science, 2003. **89**(2): p. 340-348.
54. Zhang, H., et al., *Gel polymer electrolyte-based on PVDF/fluorinated amphiphilic copolymer blends for high performance lithium-ion batteries.* RSC Advances, 2014. **4**(64): p. 33713-33719.
55. Fang, L.-F., et al., *Improving the wettability and thermal resistance of polypropylene separators with a thin inorganic-organic hybrid layer stabilized by polydopamine for lithium ion batteries.* RSC Advances, 2014. **4**(43): p. 22501-22508.
56. Sousa, R.E., et al., *Influence of the porosity degree of poly(vinylidene fluoride-co-hexafluoropropylene) separators in the performance of Li-ion batteries.* Journal of Power Sources, 2014. **263**(0): p. 29-36.
57. Hassoun, J., et al., *A New, Safe, High-Rate and High-Energy Polymer Lithium-Ion Battery.* Advanced Materials, 2009. **21**(47): p. 4807-4810.
58. Costa, C.M., et al., *Influence of different salts in poly(vinylidene fluoride-co-trifluoroethylene) electrolyte separator membranes for battery applications.* Journal of Electroanalytical Chemistry, 2014. **727**(0): p. 125-134.